ARMY RESEARCH LABORATORY

Application of an Arbitrary Lagrangian Eulerian Method to Describe High Velocity Gas-Particle Flow Behavior

D. M. Fox and J. S. Lee

ARL-RP-338   **September 2011**

NOTICES

Disclaimers

The findings in this report are not to be construed as an official Department of the Army position unless so designated by other authorized documents.

Citation of manufacturer's or trade names does not constitute an official endorsement or approval of the use thereof.

Destroy this report when it is no longer needed. Do not return it to the originator.

Army Research Laboratory
Aberdeen Proving Ground, MD 21005-5066

ARL-RP-338 September 2011

Application of an Arbitrary Lagrangian Eulerian Method to Describe High Velocity Gas-Particle Flow Behavior

D. M. Fox
Weapons and Materials Research Directorate, ARL

J. S. Lee
Wayne State University

REPORT DOCUMENTATION PAGE

Public reporting burden for this collection of information is estimated to average 1 hour per response, including the time for reviewing instructions, searching existing data sources, gathering and maintaining the data needed, and completing and reviewing the collection information. Send comments regarding this burden estimate or any other aspect of this collection of information, including suggestions for reducing the burden, to Department of Defense, Washington Headquarters Services, Directorate for Information Operations and Reports (0704-0188), 1215 Jefferson Davis Highway, Suite 1204, Arlington, VA 22202-4302. Respondents should be aware that notwithstanding any other provision of law, no person shall be subject to any penalty for failing to comply with a collection of information if it does not display a currently valid OMB control number.
PLEASE DO NOT RETURN YOUR FORM TO THE ABOVE ADDRESS.

1. REPORT DATE *(DD-MM-YYYY)*	2. REPORT TYPE	3. DATES COVERED *(From - To)*
September 2011	Reprint	24–29 July 2011

4. TITLE AND SUBTITLE	5a. CONTRACT NUMBER
Application of an Arbitrary Lagrangian Eulerian Method to Describe High Velocity Gas-Particle Flow Behavior	
	5b. GRANT NUMBER
	5c. PROGRAM ELEMENT NUMBER

6. AUTHOR(S)	5d. PROJECT NUMBER
D. M. Fox and J. S. Lee[*]	
	5e. TASK NUMBER
	5f. WORK UNIT NUMBER

7. PERFORMING ORGANIZATION NAME(S) AND ADDRESS(ES)	8. PERFORMING ORGANIZATION REPORT NUMBER
U.S. Army Research Laboratory ATTN: RDRL-WMP-F Aberdeen Proving Ground, MD 21005-5066	ARL-RP-338

9. SPONSORING/MONITORING AGENCY NAME(S) AND ADDRESS(ES)	10. SPONSOR/MONITOR'S ACRONYM(S)
	11. SPONSOR/MONITOR'S REPORT NUMBER(S)

12. DISTRIBUTION/AVAILABILITY STATEMENT

Approved for public release; distribution is unlimited.

13. SUPPLEMENTARY NOTES

A reprint from the *Proceedings of ASME-JSME-KSME Joint Fluids Engineering Conference*, Hamamatsu, Shizuoka, Japan, 24–29 July 2011.

[*]Wayne State University, Detroit, MI 48202

14. ABSTRACT

Novel computational and small-scale experimental investigations were performed in order to better understand the high velocity flow behavior of gas-particle mixtures. The motion of solid objects impacted by the flow of the mixtures was measured by use of high-speed digital video photography. Computations were performed by use of an arbitrary Lagrangian Eulerian (ALE) treatment in a nonlinear finite element code. Constitutive models for description of the solid component of the gas-particle blend were developed based on quasi-statically determined test results. It was observed that there was very close agreement between experimental and computational results and that it was possible to accurately predict the high velocity flow behavior of the gas-particle mixture using quasi-statically determined constitutive models.

15. SUBJECT TERMS

mine blast, shallow buried explosive, small-scale experiments, soil model, computation mechanics, arbitrary Lagrangian-Eulerian method

16. SECURITY CLASSIFICATION OF:			17. LIMITATION OF ABSTRACT	18. NUMBER OF PAGES	19a. NAME OF RESPONSIBLE PERSON David M. Fox
a. REPORT	**b. ABSTRACT**	**c. THIS PAGE**	UU	14	**19b. TELEPHONE NUMBER** *(Include area code)*
Unclassified	Unclassified	Unclassified			410-278-6033

AJK2011-03075

APPLICATION OF AN ARBITRARY LAGRANGIAN EULERIAN METHOD TO DESCRIBE HIGH VELOCITY GAS-PARTICLE FLOW BEHAVIOR

D. M. Fox
US Army Research Laboratory
Aberdeen Proving Ground, MD, USA

J. S. Lee
Wayne State University
Detroit, MI, USA

ABSTRACT

Novel computational and small-scale experimental investigations were performed in order to better understand the high velocity flow behavior of gas-particle mixtures. The motion of solid objects impacted by the flow of the mixtures was measured by use of high-speed digital video photography. Computations were performed by use of an arbitrary Lagrangian Eulerian (ALE) treatment in a nonlinear finite element code. Constitutive models for description of the solid component of the gas-particle blend were developed based on quasi-statically determined test results. It was observed that there was very close agreement between experimental and computational results and that it was possible to accurately predict the high velocity flow behavior of the gas-particle mixture using quasi-statically determined constitutive models.

INTRODUCTION

Full-scale vehicle blast tests are relatively expensive. However, computational and small-scale experimental methods can be employed to gain deeper insight into the mechanics of phenomena that involve the interactions between explosives, geomaterials, and solid bodies that are excited by such multi-component systems. Many experimental techniques, analytical methods, and correlations for the description of blast events and for the prediction of structural response to blast inputs have been developed over the years. Baker [1] assembled an excellent review of experimental and theoretical results relating to air blast. Kinney and Graham [2] collected and compiled air blast data from various sources. Based on these data, they showed empirical formulations for the prediction of air blast phenomena. Westine et al. [3] performed tests with measurement of impulse imparted to flat plates from explosives buried in soil and, based on the results, developed an empirical correlation for the prediction of structural excitation from blasts from shallow buried explosives.

It has been shown that small-scale experimental results can closely match those for full-scale tests [4-6]. Genson [7] performed small-scale blast tests on rigid aluminum plates.

Various researchers have applied computational techniques for treatment of the behavior of explosive, soil, and target in mine blast situations. Laine and Sandvik [8] developed a constitutive model that has been used as the basis for definition of the behavior of sand. Szymzcak [9] applied a viscoplastic model for soil and used a generalized hydrodynamic numerical formulation in order to predict the response of flat plates to excitation from explosives buried in wet sand. It was observed that this computational approach matched experimental results very well as long as the ratio of target height above the ground to depth of burial was three or less. Grujicik et al. [10-11] have investigated the use of various soil constitutive models with incorporation of porosity effects. More recently, Deshpande et. al. [12] have proposed a novel approach to modeling the soil that takes into account various regimes of soil behavior that evolve during the course of the detonation event. Neuberger et al. [13] examined the scaling of flat plate deformation with excitation from large explosive charges flush buried in dry sand, by means of a combination of experiment and computation. The computation agreed well with experiment and was performed using an arbitrary Lagrangian-Eulerian technique with the dry sand modeled by means of a generalized Mohr-Coulomb model.

Finally, Williams et al. [14] used a Lagrangian method, with soil and explosive modeled with a particle technique and soil behavior prescribed using a hybrid elastic plastic model, to predict the response of a flat target to the blast from a shallow buried explosive. Three types of soil were modeled – dry sand, a mix of clay and sand, and a wet clay – and although direct correlations to experiment were not presented, computational results followed the expected trend, viz., the impulse imparted to the target increased with decreasing soil compressibility and yield strength.

In the present work, experimental results from small-scale tests performed by Fourney et. al. [15] are compared with computational investigations in order to gain deeper insight into the physics behind the excitation of rigid targets. The targets used for this work were disk-shaped, relatively rigid, aluminum

targets and were excited by explosive buried in water, wet sand, or dry sand.

EXPERIMENTAL PROCEDURES

Figure 1 illustrates the experimental setup used by Fourney et. al. [15] to measure the response of the rigid aluminum plates to the excitation of shallow buried explosive.
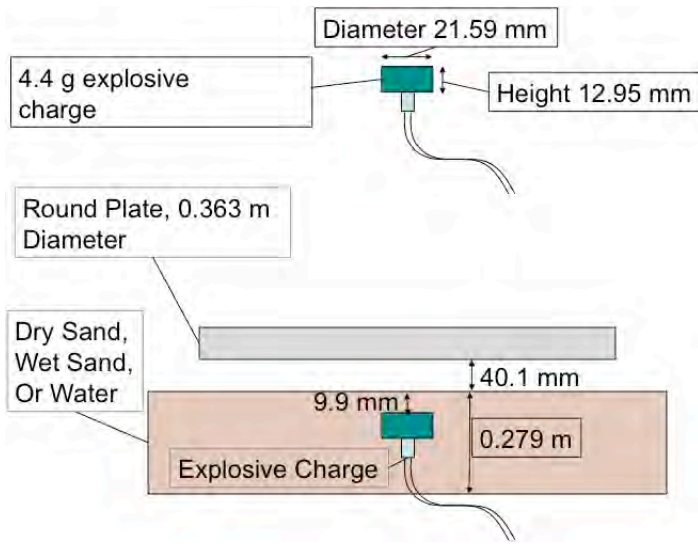

FIGURE 1. EXPERIMENTAL SETUP USED BY FOURNEY ET. AL. [15] TO MEASURE ALUMINUM PLATE RESPONSE TO EXCITATION FROM SHALLOW BURIED EXPLOSIVE.

The 4.4 g explosive charges used for this work were constructed using Detasheet C and an RP-87 detonator. The cylindrical charges were inserted into a bed of water, wet sand, or dry sand so that their top faces were 9.9 mm below the top surface of the bed. The bottom face of the aluminum target plate was located 40.1 mm above the top surface of the bed. The plate was constructed of aluminum alloy 6061 with mass 10.05 kg and behaved essentially as a rigid body in its response to the loading from the buried explosive. Impulse on target was measured by tracking the motion of the target using high-speed video.

COMPUTATIONAL PROCEDURES

Often, it is considered that computations involving solid mechanics are best performed using a Lagrangian description of the problem with a computational mesh that moves with the solid material. Computations involving fluids are most often performed using an Eulerian description with a mesh that is fixed in space. As a result of the nature of the current problem, which involves coupling between fluid and solid constituents, computations were here performed using an ALE approach for the fluids coupled with a Lagrangian approach for the solid target. If a purely Lagrangian finite

element approach had been used, this would have been an appropriate choice for the solid mechanics part of the problem, but mesh distortion resulting from large displacements caused by the explosive and fluid motions would have caused the calculations to become unstable. An Eulerian approach would have been a good choice of continuum treatment for the explosive and the fluid components but the accuracy of the treatment of the solid target would have been sacrificed. The ALE approach used here offers the advantages of the moving mesh for handling the transport of mass, momentum, and energy for the fluid constituents and can be easily coupled, via a penalty coupling algorithm, to the solid target, which is given a purely Lagrangian treatment.

Given a moving mesh such as the one that is used for the ALE computations, the conservation equations, neglecting thermal effects, for the transport of mass, momentum, and energy, respectively, are

$$\frac{\partial \rho}{\partial t} = -\rho v_{i,i} - (v_i - u_i) \rho_{,i} \tag{1}$$

$$\rho \frac{\partial v_i}{\partial t} = t_{ji,j} + \rho b_i - \rho (v_i - u_i) v_{j,i} \tag{2}$$

$$\rho \frac{\partial e}{\partial t} = t_{ij} d_{ij} + \rho b_i v_i - \rho (v_i - u_i) e_{,i} \tag{3}$$

where ρ is the mass density, u_i the mesh velocity vector, v_i the material velocity vector, t_{ij} the stress tensor, b_i the body force vector, e the internal energy, d_{ij} the rate of deformation tensor, and where, for any quantity Q,

$$Q_{,i} \equiv \frac{\partial Q}{\partial x_i} \tag{4}$$

Computations involving the explosive detonation products, air, and bed material – either wet sand, dry sand, or water - were performed numerically by means of a multi-material arbitrary Lagrangian-Eulerian (ALE) technique as implemented in the LS-DYNA explicit finite element solver [16]. LS-DYNA version 971 R4.2.1 was used for this work. The behavior of the materials that were handled using the ALE method and the behavior of the aluminum target, treated by means of explicit Lagrangian finite element calculations, were coupled by means of a penalty method.

The ALE calculations were performed as follows. For each time step, a split operator technique was used to solve the transport equations for the mass, momentum, and energy transport of the air, detonation product, and soil constituents, that is to say the ALE constituents, of the problem. First, there was a Lagrangian step that involved an explicit finite element approach to the solution of the conservation equations. The

masses of all constituents of the ALE domain was located at the nodes. These masses, in conjunction with applied forces and the momentum balance were used to calculate the nodal accelerations. These accelerations were then used to calculate velocities and displacements. Subsequently a new, more uniform, mesh was created by the solver and then, finally, for each time step, momentum, mass, and energy for each species were advected from the old Lagrangian mesh into the newly created Lagrangian mesh. The donor cell algorithm, a first order upwind scheme, was used to perform the advection step [17]. For each time step, the temporal integrations were performed explicitly using a second order accurate central differencing scheme.

For the purposes of the present work, the description of the multi-phase mixture of detonation products, soil, and air was handled in a relatively simple manner that is often used for ALE computations. Each element within the ALE computational domain could be populated with more than one material. For each time step, the strain rates for all materials within an element were set to the value of the average strain rate for the element. Subsequently, the stress state of each element was determined by summing the products of the volume fraction and stresses of each constituent of the element. Beyond this, no assumptions were made regarding the coupling of the soil and gaseous components of the mixture. Benson [18] has reported that this method, is simple, robust, and conserves energy exactly. It is expected that future investigation will include a comparison of the present approach with some of the more traditional approaches to coupling between gaseous components and solid particles.

The interface between the rigid target and the fluids was treated as having infinite slip. At the outer surfaces of the computational domain the default zero force boundary condition was used. For this boundary condition, outflow is not prevented and inflow to cells is constrained to be composed of the same material that is present in the cells [19].

The 6061 aluminum alloy that comprised the targets was modeled as a rigid solid. The behavior of the reaction products from the detonation of Detasheet C, the high explosive used for this work, was defined in terms of initial density, Chapman-Jouget pressure, detonation velocity, and a Jones Wilkins Lee (JWL) equation of state for description of the adiabat. The form of the JWL equation of state that was used for this work was

$$p = A\left(1 - \frac{\omega}{R_1 V}\right)e^{-R_1 V} + B\left(1 - \frac{\omega}{R_2 V}\right)e^{-R_2 V} + \frac{\omega E'}{V} \quad (5)$$

V in this equation is defined as the ratio of the volume of the detonation reaction products to the initial volume of the explosive; E' is the energy per unit volume; p is the pressure. A, ω, R_1, B, and R_2 are constants available along with the Chapman-Jouget parameters, for many explosives, from various sources. The air was modeled as a fluid with Newtonian viscosity and an ideal gas equation of state

$$p = \rho\left(C_p - C_v\right) T \quad (6)$$

where ρ is the density and T is the absolute temperature. C_p and C_v, represent the specific heat at constant pressure and at constant volume, respectively.

The behavior of shallow buried explosives in soil is dependent not only on the characteristics of the high explosive but is also very much a function of the properties and moisture content of the soil in which the explosives are buried. The definition of the properties of wet and dry sand as applied in this work was based on some of the standard definitions of soil constitutive properties as found in, e.g., Chen and Baladi [20], and generated for the work that was done to develop hybrid elastic-plastic soil models which were implemented for use in the SABER code, developed by the US Engineer Research and Development Center in conjunction with Titan Research and Technology, for the prediction of ground shock [21]. Strength and failure relations were developed for the SABER code based on quasi-static test results.

The compressive strength relation, failure surface, and other physical soil parameters used for the wet sand were developed using an iterative linear interpolation process and were subsequently validated successfully against small-scale blast experiments for an, as yet, unpublished report. Starting with the available material parameters from physical tests for concrete sand with 1 and 5 percent air filled voids, the LS-DYNA material model *MAT_PSEUDO_TENSOR and equation of state *EOS_TABULATED_COMPACTION were used to calculate impulsive loading on a flat target using the LS-DYNA ALE technique for each of the two levels of porosity.
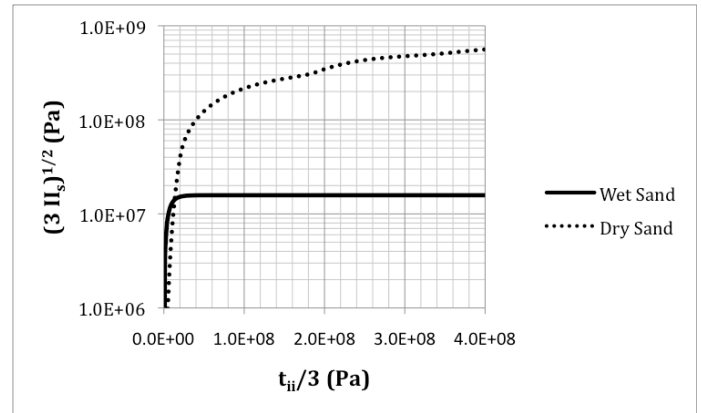

FIGURE 2. FAILURE SURFACES FOR WET AND DRY SAND.

Subsequently a simple bisection method was used to iteratively perform linear interpolation of all soil model constants until the LS-DYNA impulse result converged to the

experimental impulse value. The experiments used previously for validation of the wet sand material model were in some respects similar to the current experiments but it should be noted that the scale and target geometry for those experiments was significantly different from those employed in the current work. The physical properties used to model the dry sand were based on the hybrid elastic-plastic models used in SABER [20].

The deviatoric, perfectly plastic failure surfaces of the soil models used to populate the LS-DYNA models for the wet and dry sand are shown in Fig. 2. II_s is the second invariant of the deviatoric stress tensor s_{ij} and is defined as

$$II_s = \frac{1}{2} s_{ij}\, s_{ij} \;. \tag{7}$$

The abscissa, $t_{ii}/3$, represents the mean compressive stress where t_{ii} is defined as the Cauchy stress tensor.

The mean normal compressive stress – volumetric strain behavior of the wet sand is given in Fig. 3 which shows the variation of mean compressive stress as a function of volumetric strain for wet concrete sand with air filled voids content at a level between 1 and 5 percent. For the purposes of this work, the volumetric strain ε_v was defined as

$$\varepsilon_v = -\ln\!\left(\frac{V}{V_0}\right), \tag{8}$$

the negative value of the natural logarithm of the relative volume. These data were used, in tabular form, to populate the LS-DYNA material models for the wet and dry sand. The soils were modeled as having densities of 2,145 and 1,750 kg/m^3, respectively, for the wet and dry sand.

The water was modeled as having a simple Newtonian dynamic viscosity of 8.684 X 10^{-4} (N s)/(m^2) and a density of 998 kg/m^3. The approach to the model for the water equation of state was based essentially on what was reported and used by Steinberg for modeling spherical explosions in water [22]. The Mie-Gruneisen equation of state was used to model the compressive behavior of the water. This equation can be written as

$$p = \frac{\rho_0\, C^2\, \mu \left[1 + \left(1 - \frac{\Gamma_0}{2}\right)\mu - \frac{a}{2}\,\mu^2 \right]}{\left[1 - \left(S_1 - 1\right)\mu - S_2\,\dfrac{\mu^2}{\mu+1} - S_3\,\dfrac{\mu^3}{(\mu+1)^2} \right]} \tag{9}$$
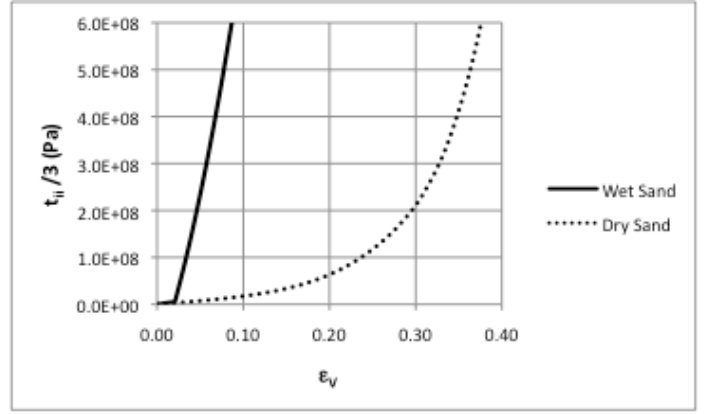

FIGURE 3. COMPRESSIVE BEHAVIOR OF WET AND DRY SAND AS A FUNCTION OF VOLUMETRIC STRAIN.

where p is the pressure, Γ_0 is the so-called Gruneisen constant, a is the linear correction to the Gruneisen constant. C, S_1, S_2, and S_3 define the intercept and the slope of the experimentally determined shock velocity – particle velocity curve for a given material. Here, the parameter μ – not to be confused with the dynamic viscosity – is defined as

$$\mu = \frac{V_0}{V} - 1 \tag{10}$$

where V/V_0 is the ratio of the volume V of the water while it is in any particular state relative to some reference volume V_0. The pressure–relative volume relation used for this work is shown graphically in Fig. 4.
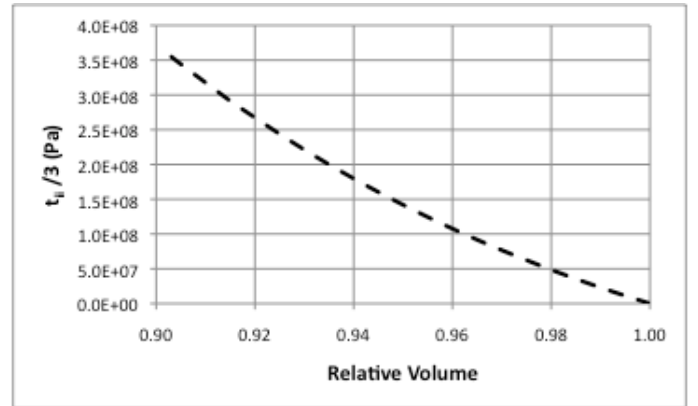

FIGURE 4. PRESSURE – RELATIVE VOLUME RELATION FOR WATER.

A cylindrical geometry was chosen for the computational domain. The mesh size for the ALE domain was varied by radial position in the circular plane of the domain. In the region closest to the center, the mesh size was 1.5-2 mm; toward the outer radius of the domain, the mesh size gradually increased to about 0.1 m. The distance between nodes in the vertical, axial, direction was approximately 2 mm but in the

domain initially filled with air gradually increased between this distance and 6.4 mm between the top of the target (in its initial position) and the top of the computational domain. The computational domain contained approximately 4 million elements.

RESULTS AND DISCUSSION

A comparison of experimental and computational results is shown in Tab. 1. An examination of these results reveals that, first of all, the computational predictions yield fairly accurate estimates of the impulse imparted to the aluminum target by means of the explosive buried in the various substrate materials. One might at first suspect that these results might have been a result of the tuning of various numerical parameters contained in the LS-DYNA solver in order to get the computation to match the experiment so closely for each of the three cases. However, beyond a mesh convergence study and the fitting, within the context of other experimental work that was done at a different scale, of the strength and failure models for the wet sand no such procedures were attempted for the purposes of the present investigation.

TABLE 1. COMPARISON OF EXPERIMENTAL AND COMPUTATIONAL RESULTS.

Substrate	Experimental Impulse (N-s)	Computational Impulse (N-s)	Percent Difference
Water	88.21	88.96	0.85%
Wet Sand	52.62	51.36	-2.40%
Dry Sand	21.13	19.69	-6.81%

It should also be noted that the material models used for the description of the sand strength and failure behavior were based entirely on quasi-static tests, viz., these material models were quite adequate for predicting impulse even though they did not account for any rate effects. This is perhaps particularly surprising since computations yielded peak particle velocities of approximately 1 km/s for the wet and dry sand substrates. The computations for the water substrate yielded peak fluid velocity of approximately 1.4 km/s.

The fact that the computational results so closely matched experiment coupled with the fact that other than the material models everything was the same between the finite element models for the wet sand, dry sand, and water systems indicates that a comparison of the material models and the impact results would be expected to uncover parametric relationships between substrate properties and the relative excitation of the aluminum target.

The densities of the water, wet sand, and dry sand were 998, 2145, and 1750 kg/m^3, respectively and the experimentally determined impulse on target was 88.21, 52.62, and 16.90 N-s, respectively, for the beds comprised of the three materials. Although the higher density wet sand bed produced higher

target momentum than the bed filled with lower density dry sand, the bed containing the lowest density material – water – was associated with the highest level of impulse. It can therefore be concluded that density was, at least for this set of soil bed substrates, not the only determinant of target loading.

A second parametric relationship is the one between failure surface and impulsive loading. Realizing that since water possesses, in its fluid state, no shear strength and comparing this result with the material models for the two sand substrates (Fig. 2), it is apparent that increasing impulse correlated, at least parametrically, with decreasing shear strength. It should be noted that there is no immediately obvious physical explanation for this relation and that, therefore, the mechanics associated with this parametric relationship will need to be examined more carefully in future work in order to determine whether this is an independent effect or whether, as suspected, these observations merely illustrate the fact that there is an incidental inverse correspondence between failure surface and mean bulk stiffness of the three substrates.

A third parametric relation is that between substrate compressive behavior and the impulse imparted to the target. In Fig. 5 a comparison is given of the relation between relative volume and pressure for each of the three bed materials.
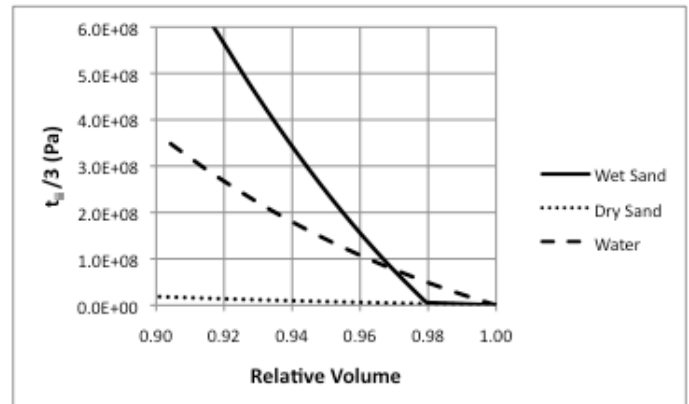

FIGURE 5. COMPRESSIVE STRESS – RELATIVE VOLUME RELATION FOR WATER, WET SAND AND DRY SAND.

The bulk stiffness of the dry sand is significantly lower than that of water. The behavior of the wet sand is a little more complicated than that of the other two materials. At lower levels of compaction, viz., between relative volumes of about 0.98 and 1.00, its compressive behavior is almost identical to that of the dry sand. However, when the wet sand is compressed beyond the point that its pores are completely filled with water its bulk stiffness, as can be seen in Fig. 3, changes radically.

Bergeron et. al. [23] report that during the course of soil-explosive blast events, and within distances of about 6 charge

radii from the center of the explosive there is a very high degree of compression of the substrate and that, beyond this distance the compression is gradually reduced. They report further that the soil laterally adjacent to and below the explosive forms something of a conduit that becomes charged with high pressure from the detonation products and, ultimately - assuming that the explosive is not too deeply buried in the substrate – ejects the cap of soil above the explosive with significant momentum.
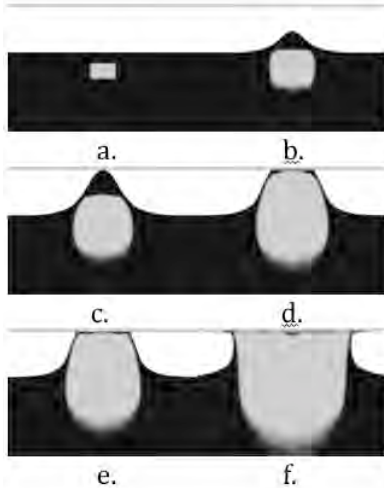

FIGURE 6. TYPICAL ALE COMPUTATIONAL EVOLUTION OF TARGET LOADING PHENOMENA. a. INITIAL STATE. b. EXPANSION OF EXPLOSIVE AND SOIL CAP. c. INITIAL CONTACT OF SOIL AND TARGET. d. CONFORMATION AT PEAK FORCE LOADING ON TARGET. e. CONFORMATION SUBSEQUENT TO PEAK LOADING WITH THINNING OF SOIL CAP. f. FURTHER SPREADING AND THINNING OF SOIL CAP.

Snapshots taken from soil volume fraction fringe plot animations developed from the wet sand computation are shown in Fig. 6. These snapshots seem to agree, at least qualitatively, with what has been observed experimentally and reported by Bergeron. Although this method shows fairly good agreement between computational and experimental impulsive loading on the target, it is clear that further work will need to be done in order to forge a more complete understanding of the aspects of this phenomenology that relate to local pressure effects.

In Fig. 6, darker fringes correspond to higher soil volume fractions. Lighter regions corresponding to lower volume fractions of soil correspond to higher volume fractions of what are, subsequent to detonation, the gaseous constituents of the ALE domain. The lower boundary of the aluminum target can be seen in each of the snapshots as a horizontal line somewhat above the upper boundary of the soil. Fig. 6a shows the initial state of the items in the computational domain: the undetonated explosive surrounded by undisturbed soil with air and the target above the soil domain. Fig. 6b, taken at 20 microseconds shows the beginning of the expansion of the detonation products and of the swelling of the soil. Fig. 6c, taken at 40 microseconds shows the initial contact between the soil cap and the target. This is the point at which the target acceleration begins to increase. Fig. 6d, is taken at 66 microseconds, the time at which the target plate acceleration reaches its peak value. Fig. 6e was taken at the point in time, 74 microseconds, at which the late acceleration suddenly dropped significantly, apparently due to a break in the soil cap. Finally, Fig. 6f shows, at 200 microseconds further spreading and thinning of the cap.
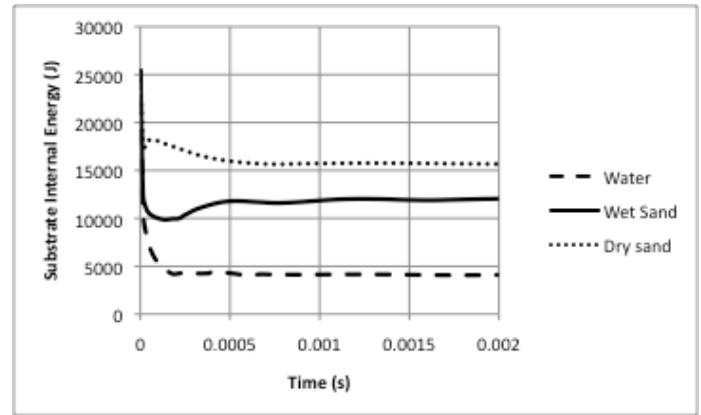

FIGURE 7. COMPUTATIONAL INTERNAL ENERGY OF WATER, WET SAND, AND DRY SAND BEDS.

In Fig. 7, the computationally determined internal energy as a function of time is presented for each of the three types of soil bed materials. The reference value of internal energy, for each substrate was chosen, for convenience, to be zero. Subsequent to the detonation it can be seen that the internal energy of the substrates rises very quickly as a result of the transfer of mechanical energy from the explosive to the substrate. The internal energy then arrives at a relatively constant value after the time reaches approximately 1 millisecond. This ultimate value of internal energy was greatest for the dry sand, somewhat lower for the wet sand, and lowest for the water so that there appeared to an inverse relation between the substrate ultimate internal energy and the amount of momentum that was transferred to the target. It seems plausible that decreasing substrate mean bulk stiffness and concomitant increased ultimate substrate internal energy would be associated with lower target momentum because more energy was expended compressing those parts of the soil bed below and laterally adjacent to the explosive, thereby making a lower proportion of the detonating explosive's mechanical energy available to drive the soil and the target which were above the explosive.

CONCLUSIONS

A comparison of experimental and computational results for impulse supplied to a rigid aluminum plate showed several things.

- It is possible to very accurately predict this sort of impulsive loading using an ALE method given appropriate material models for the explosive and bed substrates.
- Quasi-statically determined properties for wet and dry sand were adequate for prediction of the impulsive loading. This suggests that rate effects might not of primary importance for this type of work.
- Density of the substrate material was not necessarily the primary determinant of impulsive loading since the bed comprised of water – the material with the lowest density – imparted the highest loading to the target.
- Impulsive loading of the target possibly increased as a result of increasing average bulk stiffness of the substrate material. This may have allowed more kinetic energy to be directed at the target since less work was done on the portion of the substrate below as well as laterally adjacent to the explosive.
- It was not obvious whether decreasing failure stress was a cause of increasing impulse delivered to target or whether this parametric relation was simply the result of an incidental inverse correspondence between failure surface and bulk stiffness.
- Although good agreement was found between computationally and experimentally determined impulsive loading, impulsive loading is the result of integration of pressure loading.
- Integration, by its very nature, has a way of smoothing physical effects.
- This implies that a significant amount of investigation still needs to be done in order to appropriately understand the nature and effects of localized pressure loading from explosives that are shallow buried in soil and other substrates.

ACKNOWLEDGMENTS

REFERENCES

[1] Baker, W.E., 1973. *Explosions in Air*. University of Texas Press, Austin.
[2] Kinney, G. F., and Graham, K. J., 1985. *Explosive Shocks in Air*. Springer Verlag, New York.
[3] Westine, P. S., Morris, B. L., Cox, P. A., and Polch, E., 1985. Development of a Computer Program for Floor Plate Response from Land Mine Explosions, Contract Report no. 13045. U.S. Army TACOM Research and Development Center, Warren, MI.
[4] Fourney, W.L., Leiste, U., Bonenberger, R., and Goodings, D., 2005. "Explosive Impulse on Plates", *Fragblast*, **9**(1), pp. 1–17.
[5] Taylor, L. C., Skaggs, R. R., and Gault, W., 2005. "Vertical Impulse Measurements of Mines Buried in Saturated Sand", *Fragblast*, **9**(1), pp. 19–28.
[6] Taylor, L. C., Fourney, W. L., Leiste, U., and Genson, K., 2008. "Geometrical Shaping of Vehicles for Reducing Impulse From Buried Explosions". Joint Classified Bombs/Warheads & Ballistics Symposium, Monterey, CA.
[7] Genson, K., 2006. "Vehicle shaping for mine blast damage reduction". MS Thesis, University of Maryland, College Park, MD.
[8] Laine, L., Sandvik, A., 2001. "Derivation of Mechanical Properties for Sand". 4th Asia-Pacific Conference on Shock and Impact Loads on Structures, Singapore, 2001.
[9] Szymczak, W., 2005. "Platform loading from explosions in saturated sand using a visco-plastic model", *Fragblast*, **9**(4), pp. 189–203.
[10] Grujicic, M.B. Pandurangan, B., and Cheeseman, B.A., 2006. "The Effect of Degree of Saturation of Sand on Detonation Phenomena Associated with Shallow-buried and Ground-laid mines", *Shock and Vibration*, **13**, pp. 41–62.
[11] M. Grujicic, M., Pandurangan, B., Qiao, R., Cheeseman, B.A., Skaggs, R.R., and Gupta, R., 2008. "Parameterization of the Porous-Material Model for Sand with Different Levels of Water Saturation", *Soil Dynamics and Earthquake Engineering*, **28**, pp. 20–35.
[12] Deshpande, V.S., McMeeking, R.M.,Wadley, H.N.G., Evans, A.G., 2009. "Constitutive model for predicting dynamic interactions between soil ejecta and structural panels", *Journal of the Mechanics and Physics of Solids*, **57**(8), pp. 1139–1164.
[13] Neuberger, A., Peles, S., and Rittel, D., 2007. "Scaling the response of circular plates subjected to large and close-range spherical explosions. Part II: Buried charges", *Int. J. Impact Eng.*, **34**, pp. 874–882.
[14] Williams, E. M., Windham, J.E., Ehrgott, J. Q., Danielson, K. T., and Gorsich, T. J., 2008. "Effect of Soil Properties on an Above Ground Blast Environment from Buried Bare Charges". 20th Military Aspects of Blast and Shock Symposium, Oslo, Norway.
[15] Fourney, W.L., Leiste, U., Hauch, A., and Jung, D., 2010. "Distribution of Specific Impulse on Vehicles Subjected to Improvised Explosive Devices", *Blasting and Fragmentation*, **4**(2), pg. 117-135.
[16] Souli, M., 2004. "LS-DYNA Advanced Course in ALE and Fluid/Structure Coupling", Livermore Software Technology Corporation, Livermore, CA.
[17] Hallquist, J. O., 2006. "LS-DYNA Theoretical Manual", Livermore Software Technology Corporation, Livermore, CA.
[18] Benson, D. J., 2010. "Introduction to Arbitrary Langrangian-Eulerian in Finite Element Methods". In Arbitrary Lagrangian-Eulerian and Fluid-Structure Interaction, M. Souli and D. J. Benson, eds., Wiley, Hoboken, NJ, pp. 1–50.
[19] Du Bois, P., and Schwer, L., 2007. "LS-DYNA Modeling of Blast and Penetration", Livermore Software Technology Corporation, Livermore, CA.

[20] Chen, W. F., and Baladi, G. Y., 1985. *Soil Plasticity: Theory and Implementation*. Elsevier Science, New York.

[21] Zimmerman, H.D., Shimano, R. T., and Ito, Y.M., 1992. Early-Time Ground Shock from Buried Conventional Explosives: User's Guide for SABER-PC/CWE, WES IR SL-92-1, U.S. Army Corps of Engineers, Waterways Experiment Station, Vicksburg, MS.

[22] Steinberg, D.J., 1987. Spherical Explosions and the Equation of State of Water. UCID-20974, Livermore, CA.

[23] Bergeron, M.D., Walker R. and Coffey, C.G., 1998. Detonation of 100-Gram Anti-Personnel Mine Surrogate Charges in Sand; A Test Case for Computer Code Validation, DRES SR 668.

NO. OF
COPIES ORGANIZATION

  1   DEFENSE TECHNICAL
(PDF   INFORMATION CTR
only) DTIC OCA
       8725 JOHN J KINGMAN RD
       STE 0944
       FORT BELVOIR VA 22060-6218

  1   DIRECTOR
       US ARMY RESEARCH LAB
       IMNE ALC HRR
       2800 POWDER MILL RD
       ADELPHI MD 20783-1197

  1   DIRECTOR
       US ARMY RESEARCH LAB
       RDRL CIO LL
       2800 POWDER MILL RD
       ADELPHI MD 20783-1197

  1   DIRECTOR
       US ARMY RESEARCH LAB
       RDRL CIO MT
       2800 POWDER MILL RD
       ADELPHI MD 20783-1197

  1   DIRECTOR
       US ARMY RESEARCH LAB
       RDRL D
       2800 POWDER MILL RD
       ADELPHI MD 20783-1197

INTENTIONALLY LEFT BLANK.